THE JOURNAL OF COMPARATIVE NEUROLOGY 493:309–320 (2005)

Expression and Function of the Neuronal Gap Junction Protein Connexin 36 in Developing Mammalian Retina

KRISTI A. HANSEN, CHRISTINE L. TORBORG, JUSTIN ELSTROTT, AND MARLA B. FELLER*
Neurobiology Section, Division of Biological Sciences, University of California at San Diego, La Jolla, California 92093-0357

ABSTRACT

With the advent of transgenic mice, much has been learned about the expression and function of gap junctions. Previously, we reported that retinal ganglion cells in mice lacking the neuronal gap junction protein connexin 36 (Cx36) have nearly normal firing patterns at postnatal day 4 (P4) but many more asynchronous action potentials than wild-type mice at P10 (Torborg et al. [2005] Nat. Neurosci. 8:72–78). With the goal of understanding the origin of this increased activity in Cx36–/– mice, we used a transgenic mouse (Deans et al. [2001] Neuron 31:477–485) to characterize the developmental expression of a Cx36 reporter in the retina. We found that Cx36 was first detected weakly at P2 and gradually increased in expression until it reached an adult pattern at P14. Although the onset of expression varied by cell type, we identified Cx36 in the glycinergic AII amacrine cell, glutamatergic cone bipolar cell, and retinal ganglion cells (RGCs). In addition, we used calcium imaging and multielectrode array recording to characterize further the firing patterns in Cx36–/– mice. Both correlated and asynchronous action potentials in P10 Cx36–/– RGCs were significantly inhibited by bath application of an ionotropic glutamate receptor antagonist, indicating that the increase in activity was synaptically mediated. Hence, both the expression patterns and the physiology suggest an increasing role for Cx36-containing gap junctions in suppressing RGC firing between waves during postnatal retinal development. J. Comp. Neurol. 493: 309–320, 2005.

Indexing terms: gap junctions; retinal waves; retinal ganglion cells; amacrine cells; bipolar cells

Interneuronal communication via gap junctions plays a critical role in the development of neural circuits. Gap junctions have been implicated in a variety of processes, including cell differentiation (Naus and Bani-Yaghoub, 1998), apoptosis (Cusato et al., 2003; Lin et al., 1998), and pathfinding between pioneer neurons and guidepost cells (Bentley and Keshishian, 1982). In addition, gap junctions coordinate calcium transients and/or bursts of action potentials in several developing regions, including ventricular zone cells (Bittman et al., 1997), neocortex (Kandler and Katz, 1998; Peinado et al., 1993; Yuste et al., 1995), and spinal cord (Hanson and Landmesser, 2003; Personius and Balice-Gordon, 2001; Saint-Amant and Drapeau, 2001).

Here we explore the role of gap junctions in regulating spontaneous activity of the developing retina. During development, spontaneous waves of depolarization propagate across the retinal ganglion cell layer (GCL). These retinal waves are critical for the refinement of retinal projections to their primary targets in the brain (for review see Feller, 2002; Grubb and Thompson, 2004) and

Grant sponsor: National Science Foundation; Grant sponsor: Klingenstein Foundation; Grant sponsor: Whitehall Foundation; Grant sponsor: March of Dimes; Grant sponsor: McKnight Scholars Fund; Grant sponsor: National Institutes of Health; Grant number: EY13528-01A1.

Christine L. Torborg's current address is Laboratory of Cellular and Synaptic Neurophysiology, NICHD, Porter Neuroscience Research Center, Room 3C-907, 35 Lincoln Drive, MSC 3715, Bethesda, MD 20892-3715.

*Correspondence to: Marla B. Feller, Neurobiology Section 0357, UCSD, 9500 Gilman Dr., La Jolla, CA 92093-0357. E-mail: mfeller@ucsd.edu

Received 12 January 2005; Revised 28 April 2005; Accepted 8 July 2005
DOI 10.1002/cne.20759
Published online in Wiley InterScience (www.interscience.wiley.com).

may also play a role in development of the retina itself (Sernagor et al., 2001; Syed et al., 2004a). Retinal waves are characterized by increases in intracellular calcium that propagate across large regions of the retina (Feller et al., 1996; Wong et al., 1995). Bath application of a low concentration of nonspecific gap junction blockers leads to a decrease in the size and frequency of retinal waves (Singer et al., 2001; Syed et al., 2004b) and, at higher concentrations, a complete blockade of all spontaneous calcium transients (Catsicas et al., 1998; Wong et al., 1998). However, the use of general antagonists does not distinguish which retinal cell types contain the gap junctions that mediate waves. In addition, gap junction antagonists might have indirect effects (Connors and Long, 2004), such as the blockade of voltage-gated calcium channels that mediate synaptic transmission in the outer retina (Vessey et al., 2004).

An alternative approach to studying the function of gap junctions in retinal waves is to utilize mice lacking specific connexins, the basic protein unit of gap junctions. Only two connexin (Cx) types, Cx36 and Cx45, have been observed in the inner mammalian retina (Guldenagel et al., 2000; Sohl et al., 2000), implying that one of these connexins may be involved in correlating RGC firing during development. Here, we have used genetically altered mice, in which the Cx36 coding sequence has been replaced by β-galactosidase (β-gal; Deans et al., 2001, 2002), to determine both the developmental expression of Cx36 in the immature retina and the role of Cx36 in retinal waves.

Cx36 is expressed in several cell types in the adult retina, including cones (Feigenspan et al., 2004), AII amacrine cells (Feigenspan et al., 2001; Mills et al., 2001), and ON cone bipolar cells (Mills et al., 2001). With regard to functionality in the adult retina, Cx36 has been shown to be an important link in mediating the transmission of rod photoreceptor signals to RGCs (Deans et al., 2002). Additionally, Cx36 is expressed in the GCL (Deans et al., 2001, 2002; Feigenspan et al., 2004; Hidaka et al., 2002), where, in the rat, it mediates coupling between alpha-type RGCs (Hidaka et al., 2004).

Little is known about the functional role of Cx36 during development of the retina. Previously, we used a multielectrode array to record extracellularly from several RGCs simultaneously in wild-type (WT) and Cx36–/– mice (Torborg et al., 2005). In WT mice at postnatal day 4 (P4), RGCs fire bursts of action potentials that are separated by long periods of silence. In contrast, in P4 Cx36–/– retinas, there was a significant subset of RGCs (approximately 15%) that fired action potentials between bursts. By P10, most Cx36–/– RGCs exhibited action potentials between bursts. The cellular basis of this additional activity is unknown.

First, by using knockout mice, we determined the developmental expression of β-gal controlled by the endogenous Cx36 regulatory promoter elements in specific cell classes during the first 4 postnatal weeks. Second, calcium imaging revealed that the spatiotemporal properties of retinal waves in the first postnatal week Cx36–/– mice were indistinguishable from WT. Third, we explored whether the increase in action potentials in Cx36–/– mice was due to changes in synaptic transmission by comparing retinal firing patterns under different pharmacological conditions.

MATERIALS AND METHODS

Mice

The University of California San Diego Institutional Animal Care and Use Committee approved all procedures. Cx36 knockout mice in which the Cx36 coding sequence was replaced by a LacZ-IRES-PLAP reporter cassette (Deans et al., 2001) were a generous gift from David Paul (Harvard Medical School). In these mice, activation of the Cx36 promoter results in expression of the cytoplasmic protein β-gal. Therefore, neurons that would normally express Cx36 now express the β-gal reporter throughout their cytoplasmic domain.

Immunofluorescence

Mice were deeply anesthetized with halothane inhalation, and whole eyes were removed and immersion fixed at 4°C in 4% paraformaldehyde and 15% picric acid in phosphate-buffered saline (PBS; pH 8.5) overnight. Eyecups were cryoprotected in 30% sucrose with 0.1% sodium azide at 4°C, frozen in OCT compound (Ted Pella, Redding, CA) and cut into 16-μm sections with a cryostat.

Sections were washed in 1× PBS, blocked for nonspecific binding with 2% normal donkey serum, 2% bovine serum albumin (BSA), 0.3% Triton X-100 in 1× PBS for 1 hour at room temperature, then incubated overnight with primary antibody in block solution at 4°C. Several primary antibodies were used in this study. First, we used mouse monoclonal β-gal antiserum (1:1,000; G8021; Sigma, St. Louis, MO), raised against β-D-galactosidase purified from *Escherichia coli* whose isotype was determined using Sigma ImmunoType Kit (ISI-1) and by a double-diffusion immunoassay with Mouse Monoclonal Antibody Isotyping Reagents (ISO-2; Sigma's technical information). We demonstrated specificity to mouse retina by the absence of β-gal-IR in WT retina (see Fig. 1C). Second, we used rabbit disabled-1 (Dab1) antiserum (B3; 1:1,000, generously donated by Brian Howell, NINDS), raised against a GST-mDab1 fusion corresponding to residues 107–243 and affinity purified with the corresponding antigen immobilized on cyanogen bromide-activated Sepharose (Sigma; Howell et al., 1997). Specificity for mouse retina was demonstrated by the absence of labeling in Dab1–/– mice (Rice and Curran, 2001). Third, we used rabbit anti-γ-aminobutyric acid (GABA) antiserum (1:2,500; Sigma A2052), raised against GABA conjugated to BSA, affinity purified, and evaluated for specificity and activity using a dot blot immunoassay (Chemicon's technical information; Chemicon, Temecula, CA). The staining pattern observed in Cx36–/– retina was consistent with previous studies of GABAergic populations in WT retina using different antibodies (see, e.g., Havercamp and Wassle, 2000) and the identical antibody (Moon et al., 2005; Zhang et al., 2005), indicating specific staining to GABAergic neurons. Fourth, we used goat anticholine acetyltransferase (ChAT; 1:200; Chemicon AB144P), raised against human placental ChAT and affinity purified. This antibody colocalized with the antibody for vesicular acetylcholine transporter in WT mice, indicating specificity to cholinergic neurons (Bansal et al, 2000). We observed ChAT antibody labeling in Cx36–/– mice that had the typical pattern of mirror-symmetric amacrine cells described for all vertebrates (Zhou, 2001b). Fifth, we used goat antiglycine transporter 1 (glyt-1; 1:5,000; Chemicon AB1770) raised against a synthetic peptide rep-

resenting the sequence KAQIPIVGSNGSSRLQDSRI from the carboxy-terminus. The staining pattern obtained using anti-glyt-1 on tissue sections taken from the CNS corresponded to the pattern described from in situ hybridization with probes to rat GLYT1 mRNA (Chemicon's technical information). Localization was consistent with previous descriptions of glyt-1 and glycine staining in WT (Silverkamp and Wassle, 2000) and Cx36–/– retina (Deans et al., 2002).

For indirect immunofluorescence, sections were incubated for 1 hour in block solution at room temperature with the appropriate affinity-purified secondary antibody conjugated to different fluorophores including Cy3 (1:500; Jackson Immunoresearch, West Grove, PA) or Alexa 488 (1:500; Molecular Probes, Eugene, OR). No-primary contols were conducted for all experiments. The sections were then rinsed in PBS and mounted in Vectashield (Vector, Burlingame, CA).

Images were acquired with a confocal microscope (Bio-Rad MRC-1024) and a water-immersion lens (×60, numerical aperture 0.9). Excitation was at 568 nm for Cy3 and 488 nm for Alexa 488, with emission filters of 585 longpass for Cy3 and 540/40 bandpass for Alexa 488. Single optical sections of 2 μm were acquired; however, three or four 2-μm optical sections were averaged to illustrate stacks of 6–8-μm optical sections, which is about the thickness of a cell body. Sections of this thickness are unreliable for determining the colocalization of puncta, in that overlap may occur from staining originating in different focal planes. Digital images were processed in Adobe Photoshop (Adobe Systems, Inc., San Jose, CA) to enhance color and contrast. All experiments were performed on the central three sections in three different retinas.

The percentage of β-gal immunoreactive cells that were also immunoreactive for the amacrine cell marker Dab1 (see Fig. 2G) was computed per section, and the results were averaged across animals at each age. The significance was assessed by using one-way ANOVA with a post hoc Tukey test. *P* values less than 0.05 were taken as significant.

Retinal preparation for acute imaging and multielectrode array

Neonatal WT and Cx36–/– mice (postnatal days 2–4) were anesthetized with isofluorane and decapitated. Retinas were isolated in cold (4°C) artificial cerebrospinal fluid (ACSF) containing (in mM): 119.0 NaCl, 26.2 $NaHCO_3$, 11 glucose, 2.5 KCl, 1.0 K_2HPO_4, 2.5 $CaCl_2$, and 1.3 $MgCl_2$. Whole retinas were then mounted, ganglion cell side up, onto filter paper. These whole-mount preparations were kept at 32°C in ACSF incubating with 10 μM fura-2AM [Molecular Probes; 50 μg of fura-2AM dissolved in 50 μl of 2% (w/v) pluronic acid in dimethyl sulfoxide (DMSO) placed in 5 ml ACSF] bubbled with 95% O_2/5% CO_2 until use (2–6 hours). During experiments, all preparations were superfused continuously with oxygenated ACSF warmed to 32°C.

Fluorescence imaging

Images were acquired with a SIT camera (MTI 300; Dage-MTI, Michigan City, IN) and upright microscope (Axioskop FS; Zeiss, Thornwood, NY) with a 10× water-immersion objective (Neofluor; Zeiss) and continuous 380-nm illumination (OptiQuip) of fura-2 AM. Initially, a background frame was acquired that was subtracted on a pixel-by-pixel basis from all subsequent frames to create a difference image. The difference image was averaged over four video frames by a digital video processor (DVP-32; InstruTech, Port Washington, NY) and recorded onto a digital VCR (Sony) with a resolution of 60 frames/second. Fractional changes in average fluorescence intensity (ΔF/F) were monitored over a 200-μm^2 area to determine the interwave interval, which is the time elapsed between spontaneous calcium transients in a given retinal region. Wavefront velocity was analyzed in NIH Image software. First, the wave initiation point was determined by the frame in which a ΔF transient signifying a wave first appeared. Second, a line perpendicular to the direction of propagation was used to mark the wavefront in each frame. Third, the total distance between wavefronts was summed across all frames to compute distance. Finally, this total distance was divided by the total time it took the wave to propagate to determine the velocity of the wave.

The initiation rate, or the frequency of retinal wave initiations across the retina in a given time period, was calculated over a 10-minute interval. Retinal wave initiation was defined by the time point at which a ΔF/F transient first appeared signifying a wave. The initiation rate was calculated by dividing the number of retinal wave initiations by the 10-minute interval to obtain initiations/minute. The initiation rate was then normalized for retina area variations by dividing the initiation rate by the respective retinal area to obtain initiations/minute/mm^2.

Interwave interval, the time elapsed between spontaneous ΔF transients in a given retinal region, was computed from the ΔF/F curves obtained from a 200-μm^2 area recorded for 10 minutes. Student's *t*-test was used to calculate significance. *P* values less than 0.05 were taken as significant.

Multielectrode recordings and analysis

A retinal piece from either a P10 WT or a P10 Cx36–/– mouse was placed GCL down onto a flat, hexagonal array of 61 extracellular electrodes spaced 60 μm from each other, with a total diameter of 480 μm. The retina was held down on the array by placing a platinum ring on the filter paper. During recording, the retina was continuously perfused with oxygenated ACSF, and the bath temperature was maintained at 33–35°C.

Spike times, peaks, and widths were digitized with a temporal resolution of 0.05 msec (Meister et al., 1994) and then stored for off-line analysis. Spikes were manually selected from the noise based on their shape. All analysis presented here used the multiunit activity recorded on each electrode, which we did for two reasons. First, because our goal was to determine the origin of all spikes fired by RGCs, and not the spiking behavior of individual cells, we did not sort spikes into individual units. Second, sorting spikes into individual units was particularly challenging in the developing mouse retina because each electrode detects units from several RGCs that fire in simultaneous bursts during retinal waves. Quantifying multiunit activity avoids potentially biasing the results to only those cells that had discernible single units.

We computed the burst frequency ratio by dividing the number of bursts/minute on each electrode in drug by the burst frequency in control. Bursts were defined as three or more spikes occurring with an interspike interval of less than 2 seconds. The spike ratio was calculated by dividing

the number of spikes recorded in drug by the number of spikes recorded in control for each electrode. Student's *t*-test was used to calculate significance. *P* values less than 0.05 were taken as significant. All other analysis was performed in IgorPro (Wavemetrics, Inc.).

RESULTS

Cx36 expression begins during the first postnatal week and gradually increases

We used knockout mice in which the Cx36 coding sequence has been replaced by a β-gal reporter to study expression of Cx36 throughout development. The distribution of the β-gal reporter was determined by indirect immunofluorescence. At P8, β-gal immunoreactivity was detected predominantly in somata in the inner one-third of the inner nuclear layer (INL) and in processes throughout the inner plexiform layer (IPL). In addition, β-gal-immunoreactive (β-gal-IR) somata were present in the GCL, faintly in the outer one-third of the INL, and in the outer plexiform layer (OPL; Fig. 1A). These results are consistent with previous β-gal expression patterns in the adult retina (Deans et al., 2002).

Two types of controls were performed to verify that β-gal immunoreactivity was indicative of normal Cx36 expression at each age examined. First, to ensure that β-gal expression was not affected by compensation in response to a complete lack of Cx36, the pattern of β-gal expression was verified in the retinas of heterozygous mice (Cx36+/–). The immunolabeling seen in Cx36+/– retinas was similar to that in Cx36–/– retinas, suggesting that β-gal expression was not altered in Cx36–/– retinas (Fig. 1B). Second, β-gal-IR cells were not detected in WT retinas, confirming a lack of endogenous reactivity to β-gal (Fig. 1C).

To detect Cx36 expression in the developing mouse retina, a time course of immunolabeling with the β-gal antibody was performed at ages P2, P4, P8, P10, P14, and P30. β-Gal immunoreactivity was first detected at P2, when a small number of discrete puncta were localized to the GCL (Fig. 1D). At P4, additional β-gal-IR somata were seen in the proximal INL (Fig. 1E). At P2 and P4, the diffuse staining in the IPL was likely background, insofar as it was present in no-primary controls (data not shown), and there was no evidence of label using an enzymatic reaction for β-gal (Torborg et al., 2005). At P8 (Fig. 1F), the number of β-gal-IR somata in the proximal INL increased, additional immunoreactive somata were visible in the GCL and distal INL, and the OPL was faintly labeled. At P10 (Fig. 1G), β-gal-IR neurons in the distal INL and GCL increased in number. The β-gal immunoreactivity in the distal INL is likely to be bipolar cells based on the location of the somata. At P14 (Fig. 1H), β-gal-IR bipolar cells were prevalent with processes extending into both the OPL and the IPL. At P30 (Fig. 1I), high levels of β-gal immunoreactivity were present in the OPL, distal and proximal INL, and GCL. In addition, there was an increase with age in the number of β-gal-IR puncta in the IPL. These observations demonstrate that, rather than a transient expression of Cx36 in specific cell types, the adult pattern of Cx36 expression emerges through a gradual increase in expression.

β-Gal-IR somata in INL are a subset of glycinergic AII amacrine cells

Previous studies in adult rodents have demonstrated that Cx36 is expressed in AII amacrine cells (Deans et al., 2002; Feigenspan et al., 2001; Mills et al., 2001). To verify that the β-gal-IR cells in the proximal INL starting at P4 were indeed AII amacrine cells and not a cell population that transiently expressed β-gal, the monoclonal antibody, Dab1, was used to label AII amacrine cells specifically (Rice and Curran, 2000). Many Dab1-IR somata and processes were present in the proximal INL and IPL (Fig. 2B,E). The morphology, location, and density of these Dab1-IR somata are consistent with AII amacrine cell labeling (Famiglietti and Kolb, 1975).

When both β-gal and Dab1 antibodies were applied to the retina, all β-gal-IR neurons in the proximal INL were immunoreactive for Dab1; however, not all Dab1-IR AII amacrine cells were immunoreactive for β-gal, indicating that Cx36 is present in only a subset of AII amacrine cells (Fig. 2). This observation was consistent throughout development. The percentage of β-gal-IR somata to Dab1-IR somata per section was significantly lower at P4 (approximately 30%) than at all other ages, when the percentage doubled and remained consistent through P30 (Fig. 2G). At this time, we cannot rule out the possibility that the expression of Cx36 in a subset of AII amacrine cells might be due to partial penetrance of the reporter (see Discussion).

β-Gal-IR somata in the GCL are not displaced amacrine cells

We observed β-gal immunoreactivity in the GCL, consistent with previous reports (Deans et al., 2002; Degen et al., 2004; Feigenspan et al., 2004). In addition, previous studies have revealed that the processes of alpha-type RGCs colocalize with Cx36 immunoreactivity in rats (Hidaka et al., 2004) and mice (Schubert et al., 2005). It is unclear whether other cell types within the GCL also express Cx36. The GCL of mice comprises both RGCs and displaced amacrine cells (Jeon et al., 1998). Most displaced amacrine cells in the mouse retina release GABA and/or acetylcholine but not glycine (Haverkamp and Wassle, 2000). To determine whether Cx36 is expressed in displaced amacrine cells, we simultaneously labeled for β-gal and GABA, the glycine transporter glyt-1, or the acetylcholine-synthesizing enzyme ChAT.

GABA-IR somata were located throughout the GCL and inner one-third of the INL as well as in immunoreactive processes in the IPL (Fig. 3A). There was no colocalization of β-gal with GABA in the GCL, showing that the β-gal-IR somata in the GCL are not GABAergic amacrine cells. In contrast, Glyt-1-IR somata colocalized with β-gal in the proximal INL (Fig. 3B) but not within the GCL, showing that β-gal-IR somata in the GCL were not glycinergic amacrine cells. Immunolabeling for ChAT revealed immunoreactive somata in the proximal INL and in the GCL, but there was no colocalization with β-gal (Fig. 3C), demonstrating that β-gal-IR somata in the GCL were not cholinergic amacrine cells. The lack of colocalization of the β-gal antibody with amacrine cell markers suggests that the β-gal-IR somata in the GCL were RGCs.

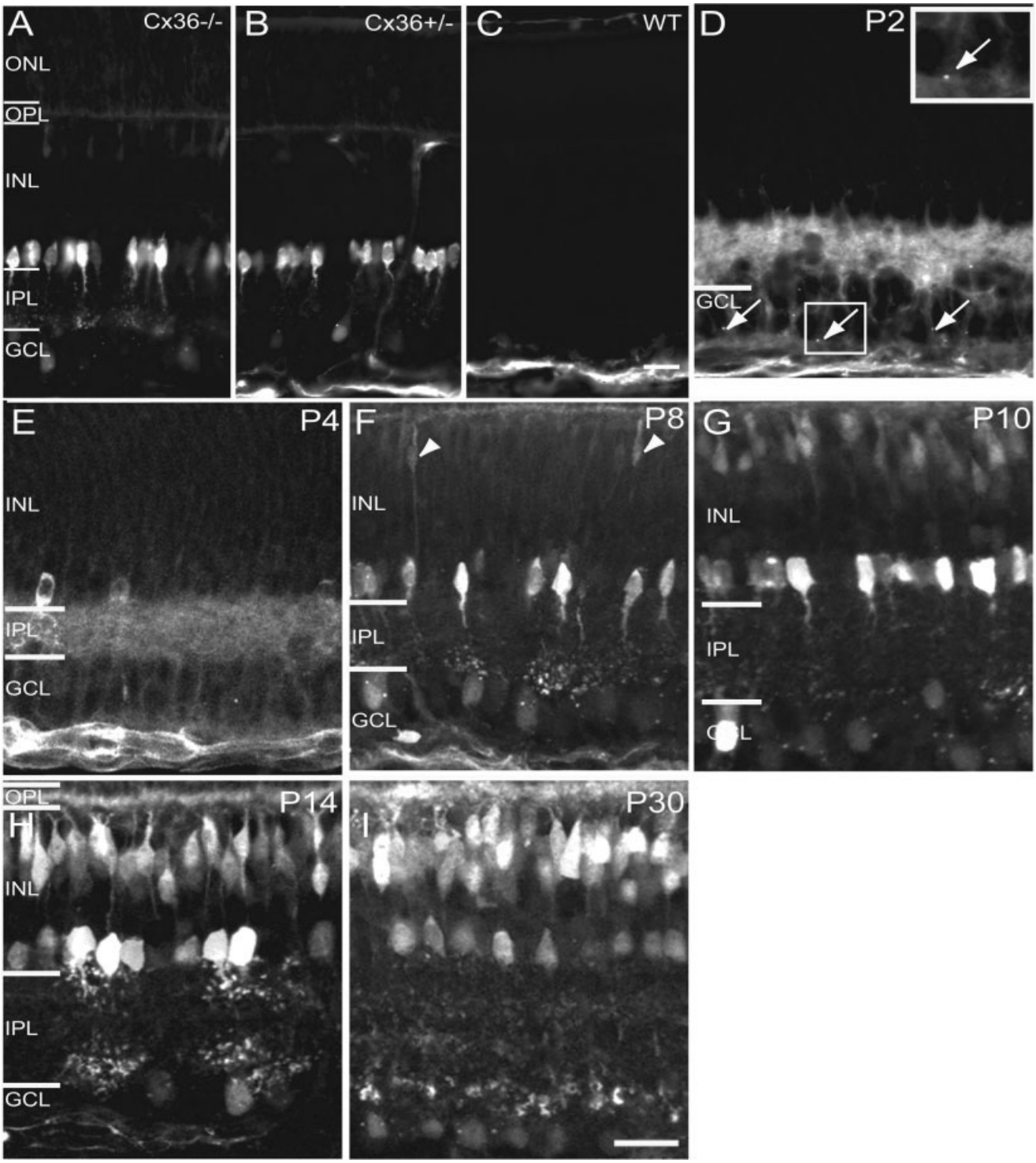

Fig. 1. β-Gal immunoreactivity during retinal development. **A–C:** Immunofluorescence of β-gal antibody at P8 in Cx36–/– (A), Cx36+/– (B), and WT (C) mice. Labeling visualized by confocal microscopy. **D–I:** Developmental expression of β-gal immunoreactivity. At P2 (D), the only detectable expression was small β-gal-IR puncta in the GCL (arrows and **inset**). At P4 (E), β-gal-IR somata were present in the proximal INL. By P8 (F), β-gal-IR somata were detected in the GCL, proximal INL, and faintly in the distal INL (arrowheads). Additional labeling was present as puncta in the proximal IPL. At P10 (G), additional β-gal antibody labeling was detected in the distal INL. By P14 (H), processes from β-gal-IR bipolar cells extended into the IPL and OPL. Processes and puncta from β-gal-IR amacrine cells extended through the IPL. At P30 (I), β-gal antibody labeling was similar to that at P14. ONL, outer nuclear layer; OPL, outer plexiform layer; INL, inner nuclear layer; IPL, inner plexiform layer; GCL, ganglion cell layer. Scale bars = 20 μm in I (applies to E–I), C (applies to A–D).

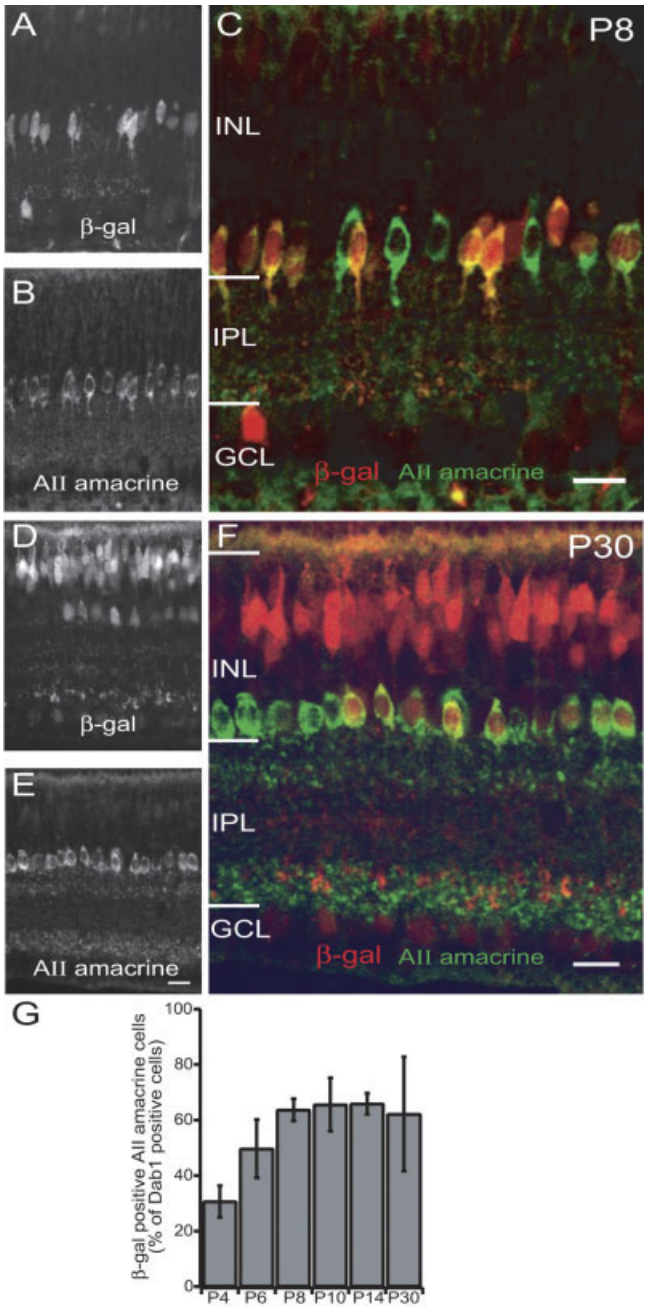

Fig. 2. Immunofluorescent identification of β-gal-immunoreactive (IR) amacrine cells with the AII amacrine cell marker Dab1. **A:** P8 Cx36–/– retinas labeled with antibodies to β-gal. **B:** P8 Cx36–/– retinas labeled with antibodies to Dab1. **C:** P8 Cx36–/– retinas doubly labeled with antibodies to β-gal (red) and Dab1 (green) showed only partial colocalization of Dab1-IR cells with β-gal IR cells. INL, inner nuclear layer; IPL, inner plexiform layer; GCL, ganglion cell layer; β-gal, β-galactosidase; Dab1, disabled-1. **D:** P30 Cx36–/– retinas labeled with antibodies to β-gal. **E:** P8 Cx36–/– retinas labeled with antibodies to Dab1. **F:** P30 Cx36–/– retinas doubly labeled with antibodies to β-gal (red) and Dab1 (green) showed only partial colocalization of Dab1-IR cells with β-gal-IR cells. **G:** Percentage of Dab1-IR somata also expressing β-gal throughout development. Percentage of β-gal-IR AII amacrine cells was significantly less at P4 than at all other ages. Error bars represent standard deviations. Scale bars = 10 μm in E (applies to A–E), C, F.

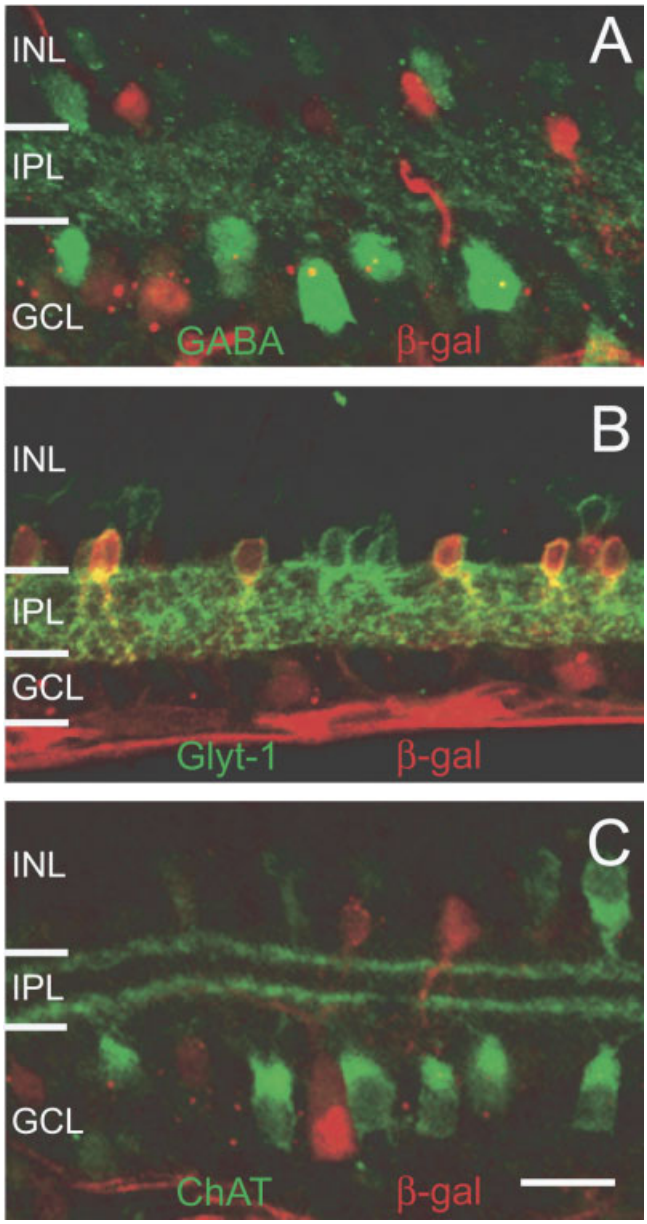

Fig. 3. Immunofluorescent identification of β-gal-IR somata in the ganglion cell layer at P8 using amacrine cell markers. Double labeling (green) GABA (**A**), glyt-1 (**B**), or ChAT (**C**) with β-gal (red) revealed no colocalization of β-gal-IR somata in the GCL. Scale bar = 10 μm in C (applies A–C).

Cx36–/– mice exhibit normal retinal waves during the first postnatal week

The observation of Cx36 expression during the age when retinal waves occur and in cell types that are involved in wave circuitry suggest a possible role for Cx36-containing gap junctions in retinal waves. To determine whether Cx36 has a role in mediating the spatial and temporal properties of retinal waves, calcium imaging was used to record the electrical activity in a neuronal population.

Fluorescent imaging of acutely isolated, fura-2-loaded WT and Cx36–/– retinas was performed during the first

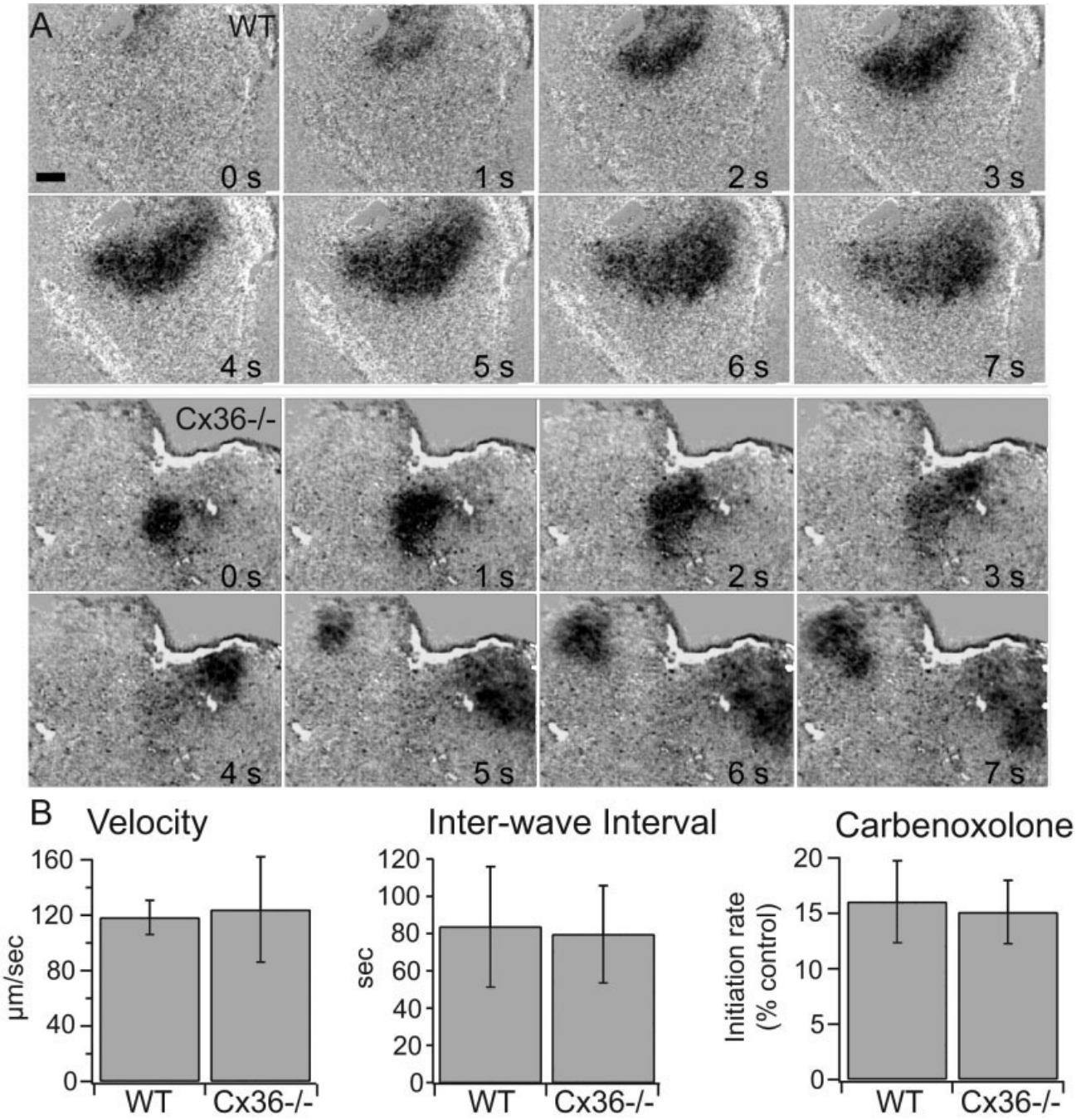

Fig. 4. Cx36 is not involved in retinal wave propagation during the first postnatal week. **A:** Propagation of retinal waves in 1-second intervals from a P3 WT retina and P2 Cx36–/– retina visualized with fluorescence imaging labeled with the calcium indicator fura-2AM. **B:** Wavefront velocity (left) and interwave interval (middle) for WT and Cx36–/– mice. Right: Initiation rate of retinal waves (waves/minute/mm^2) when carbenoxolone was bath applied to WT and Cx36–/– retinas. Error bars represent standard deviations. Scale bar = 100 μm (applies to all panels in A).

postnatal week. Retinal waves in Cx36–/– retinas were indistinguishable from those in WT in that retinal waves initiated in random locations, propagated over finite distances, and stopped at refractory boundaries (Fig. 4A). There was no significant difference between WT and Cx36–/– mouse retinas in wavefront velocity (Cx36–/– = 124.0 ± 38 μm/second, n = 30 waves; WT = 117.21 ± 22 μm/second, n = 9 waves; Fig. 4B) or interwave interval (Cx36–/– = 79.5 ± 26 second, n = 10 retinas; WT = 83.6 ± 32.3 second, n = 7 retinas; Fig. 4C), indicating that Cx36 is not involved in retinal wave propagation during the first postnatal week.

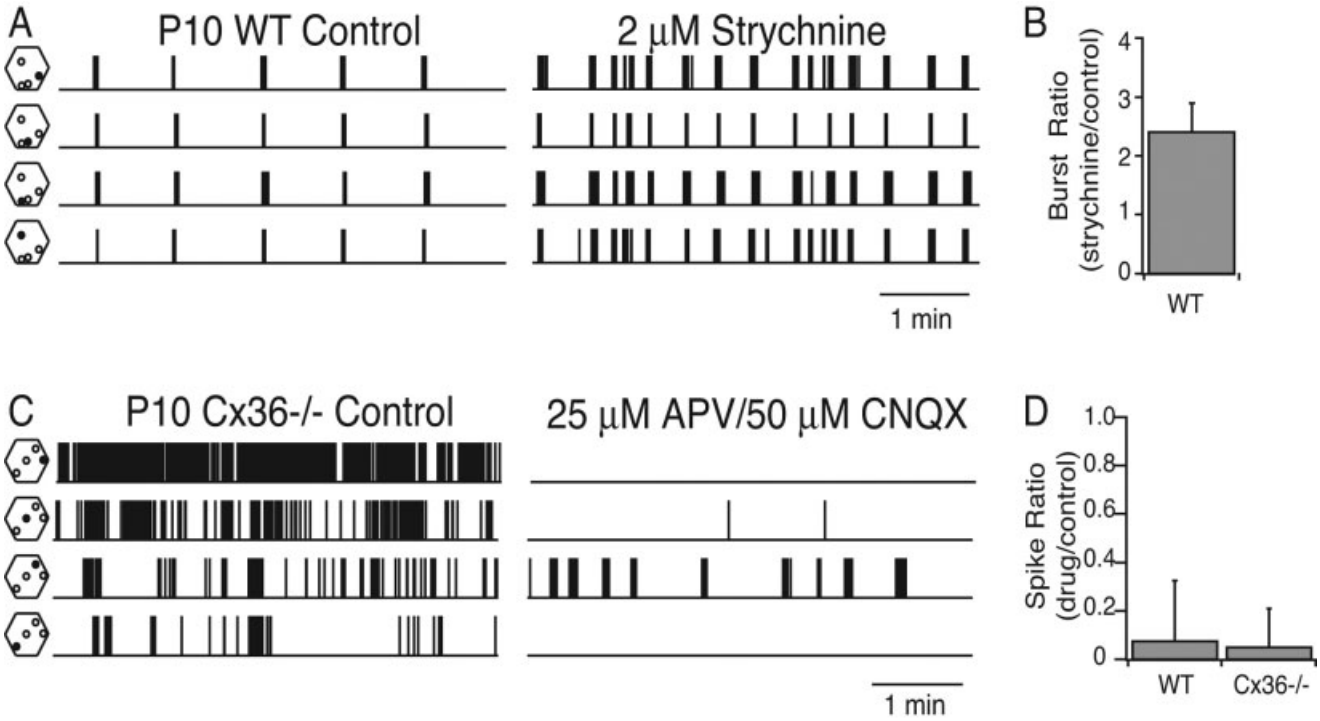

Fig. 5. Enhanced excitability of Cx36–/– RGCs is due to increased glutamatergic synaptic input and not decreased glycinergic synaptic input. **A:** Multiunit spike trains recorded from four different electrodes from a P10 WT retina in the absence (left) and presence (right) of 2 μM strychnine. Hexagons to the left of each spike train show the position (solid circle) of the electrode on the multielectrode array that recorded spikes. Total lengths of control and drug-application recordings shown here are 5 minutes each. **B:** Summary of the increase in burst frequency after the application of 2 μM strychnine. The frequency of bursts after drug application was normalized to the multiunit burst frequency before strychnine application for each electrode (n = 217 electrodes, five retinas). **C:** Multiunit spike trains recorded from four different electrodes from a P10 Cx36–/– retina in the absence (left) and presence (right) of 25 μM APV and 50 μM CNQX. Hexagons to the left of each spike train show the position (solid circle) of the electrode on the multielectrode array that recorded spikes. Total lengths of the recordings shown here are 5 minutes each. **D:** Summary of the decrease in the number of spikes after ionotropic glutamate receptor blockade for P10–11 Cx36–/– mice and P10–11 WT mice. The number of spikes recorded on each electrode after application of antagonists (25 μM APV and either 50 μM CNQX or 10 μM NBQX) was normalized to the number of spikes recorded on that electrode before drug application (Cx36–/– mice: n = 83 electrodes, two retinas; WT mice: n = 226 electrodes, four retinas). The results were not signficantly different ($P = 0.3$).

To verify that gap junctions other than Cx36 contribute to the propagation of retinal waves, the gap junction blocker carbenoxolone (100 μM) was bath applied to P2–P4 WT and Cx36–/– retinas. In the presence of carbenoxolone, both WT and Cx36–/– retinas exhibited a significant decrease in the total area covered by individual retinal waves (data not shown). Waves initiated at various locations in the retina but did not propagate. Because retinal waves did not propagate and the areas were small, interwave interval could not be measured; therefore, initiation rate was used as a measure of retinal wave frequency. In both WT and Cx36–/– retinas, carbenoxolone caused a decrease in the initiation rate of waves (number of waves/minute/mm^2) compared with controls (Fig. 4B). These findings suggest that either another connexin is involved in mediating retinal activity during the first postnatal week or carbenoxolone is blocking retinal wave propagation via a nonspecific action.

Altered firing patterns in Cx36–/– retinal neurons can be attributed to an increase in excitatory synaptic inputs

Although no differences were detected in the spatial and temporal properties of retinal waves during the first postnatal week in Cx36–/– mice, the expression pattern suggested a role for Cx36 later in development. Because the techniques used to load the retina with AM-calcium indicators in the second week disrupt the spatial pattern of activity (Bansal et al., 2000), we assayed firing patterns on P10 Cx36–/– mice with a multielectrode array, which allowed us to record extracellularly from many cells simultaneously (Meister et al., 1991; Wong et al., 1993).

At P4 and P10, WT retinal neurons fire bursts of action potentials that are correlated with action potentials from neighboring cells and are followed by long periods of silence (Fig. 5A). At P4, Cx36–/– retinal neurons have normal firing patterns, although a small percentage exhibits an increased number of action potentials between correlated bursts (Torborg et al., 2005). In contrast, most Cx36–/– retinal neurons at P10 fire many action potentials between correlated bursts (Torborg et al., 2005; Fig. 5C).

The increase in action potential firing in Cx36–/– mice might be due to a decrease in inhibitory synaptic input, an increase in excitatory synaptic input, or an increase in the excitability of RGCs. Cx36 is highly expressed in AII amacrine cells, which have a glycinergic input onto OFF cone bipolar cells (Pourcho and Goebel, 1985). Hence the ap-

parent disinhibition of RGC firing could be a result of a lack of glycine secretion. To test this hypothesis, we bath applied the glycine receptor antagonist strychnine (2 μM) to P10 WT retinas. This resulted in a 2.5–3-fold increase in burst frequency (Fig. 5A,B) but did not result in increased firing between bursts as observed in Cx36–/– retinas (Fig. 5C). These findings are consistent with the increase in retinal wave frequency after application of strychnine to rabbit retina (Zhou, 2001a). Thus, the increase in the number of action potentials observed in Cx36–/– is not due to a complete lack of glycine signaling.

Cx36 is highly expressed in bipolar cells, the primary source of glutamatergic input to the majority of amacrine cells and RGCs. To test whether the increase in action potential firing in Cx36–/– mice is due to an increase in excitatory synaptic input, we bath applied the ionotropic glutamate receptor antagonists CNQX (50 μM) or NBQX (10 μM) and APV (25 μM). Blockade of ionotropic glutamate receptors resulted in a dramatic decrease in the firing of action potentials in P10 Cx36–/– retinas (Fig. 5C,D), similar to the blockade observed in P10–11 WT mice (Fig. 5D). Hence, we conclude that the activity in Cx36–/– mice was driven primarily by the synaptic release of glutamate from bipolar cells.

DISCUSSION

We have characterized the expression and function of Cx36 in the developing inner retina by using a knockout mouse in which the Cx36 gene was replaced by a β-gal reporter. We found that expression of Cx36 throughout the INL and IPL steadily increased until reaching adult-like patterns at P14. Cx36 expression was observed in AII amacrine cells, bipolar cells, and RGCs, confirming previous studies (Deans et al., 2002; Feigenspan et al., 2001, 2004; Mills et al., 2001). Finally, Cx36 was not necessary for the propagation of retinal waves during the first postnatal week but regulated the firing properties of individual RGCs, most dramatically during the second postnatal week. The increase in action potential firing observed in Cx36–/– RGCs likely was due to an increase in the amount of glutamatergic synaptic release from bipolar cells or an increase in RGC excitability rather than a decrease in glycinergic release from AII amacrine cells.

Developmental expression of Cx36 and implications for functional coupling

Cx36 is expressed throughout the central nervous system (Belluardo et al., 2000; Condorelli et al., 1998, 2000; Deans et al., 2002; Feigenspan et al., 2001; Mills et al., 2001; Rash et al., 2000; Sohl et al., 1998), where it coordinates activity among populations of neurons (Buhl et al., 2003; Deans et al., 2001; Long et al., 2002). Cx36 is hypothesized to play a transient role during development, because its expression peaks in the neocortex, thalamus, hypothalamus, and hippocampus during the first 3 postnatal weeks and declines thereafter (Belluardo et al., 2000; Ben-Ari et al., 2004). However, we found no evidence in the retina for a transient expression of Cx36 during development. Instead, Cx36 reporter expression in the retina gradually increased from its initially low levels at P4 until reaching an adult-like pattern and level of expression at P14 (Fig. 1).

For the developing INL, we detected Cx36 expression in AII amacrine cells (starting at P4) and bipolar cells (starting at P8). This pattern of expression was similar to that found in previous studies in the adult INL, in which Cx36 has been localized to AII amacrine cells and at least two types of cone bipolar cells (Deans et al., 2002; Feigenspan et al., 2001; Mills et al., 2001). Because the cell types that express Cx36 are similar in both the immature and the adult retina, we hypothesize that neonatal functional coupling mediated by Cx36 is located between the same junctions as in adult. In the adult inner retina, functional coupling has been observed between pairs of AII amacrine cells and AII amacrine and ON cone bipolar cells (Veruki and Hartveit, 2002a,b).

Previous studies with Cx36–/– mice showed the colocalization of β-gal with glyt-1, indicating that Cx36 is present in the glycinergic AII amacrine cells (Deans et al., 2002), yet eight different types of glycinergic amacrine cells can be distinguished in the INL (Menger et al., 1998). Therefore, Dab1 is a more precise marker for AII amacrine cells than glyt-1 (Rice and Curran, 2000). We used double labeling to reveal that all β-gal-IR somata were also immunoreactive for the AII amacrine cell marker Dab1, indicating that AII amacrine cells are the only type of amacrine cell containing Cx36. However, Cx36 is expressed in approximately 60% of Dab1-IR AII amacrine cells. This observation means either that not all AII amacrine cells form Cx36-containing gap junctions or that there was variable or incomplete reporter expression. Indeed, partial penetrance of the PLAP reporter into Cx36-containing retinal neurons was previously reported (Deans et al., 2002).

Cx36–/– expression in bipolar cells became visible at P8 and increased in expression through P30 (Fig. 1). In adult rodents and rabbits, Cx36 is not found in rod bipolar cells (Deans et al., 2002; Feigenspan et al., 2001, 2004; Mills et al., 2001); however, it is present in both OFF cone bipolar cells (Deans et al., 2002; Feigenspan et al., 2004) and ON cone bipolar cells (Deans et al., 2002). In the rat, ON cone bipolar cell terminals labeled with recoverin appear in the IPL at P8 and do not become distinct until P12 (Gunhan-Agar et al., 2000), suggesting that Cx36-containing gap junctions may be present as bipolar cell axons mature. Glycine is known to diffuse from AII amacrine cells to ON cone bipolar cells via heterologous gap junctions (Vaney et al., 1998). Previous studies have shown that glycine-IR ON cone bipolar cells first appear at P10 and dramatically increase in numbers until P14 in rat retinas (Pow and Hendrickson, 2000). Therefore, by P10, AII amacrine cells may form functional gap junctions with ON cone bipolar cells. In Cx36–/– mice, glycine cannot be detected in ON cone bipolar cells, indicating the gap junction between AII amacrine cells and ON cone bipolar cells contains Cx36 (Deans et al., 2002). This later expression of Cx36 in bipolar cells is consistent with our observation that the increased number of action potentials in Cx36–/– RGCs is driven by an increase in glutamatergic transmission (Fig. 5C,D).

In the GCL, Cx36 expression first appeared in somata at P8. Double labeling of the β-gal antibody with GABA, glyt-1, or ChAT antibodies revealed no colocalization of β-gal with any of the amacrine cell markers (Fig. 3). This suggests that the Cx36-containing cell type in the GCL is an RGC. Previous studies using Cx36–/– mice have also observed β-gal-IR somata within the GCL that resembled RGCs in both size and number (Degen et al., 2004; Feigenspan et al., 2004).

Cx36 regulation of spontaneous activity in developing RGCs

Retinal waves are mediated by several different mechanisms working in concert (for review see Zhou, 2001b). The evidence for a role of gap junctions is twofold. First, during early postnatal development, strong tracer coupling is observed between select cell types within the inner retina (Catsicas et al., 1998; Penn et al., 1998; Singer et al., 2001). Second, bath applications of pharmacological agents known to inhibit coupling also inhibit waves (Catsicas et al., 1998; Singer et al., 2001; Wong et al., 1998). Unfortunately, use of pharmacology to assay the role of gap junctions is difficult, because most of the agents are nonspecific. Gap junction antagonists may disrupt non-gap junction membrane proteins that affect the excitability of neurons (Deans et al., 2001; Long et al., 2002) or inhibit voltage-gated calcium channels that mediate synaptic transmission (Vessey et al., 2004). Use of a dosage that inhibits functional coupling between RGCs but maintains normal firing response to step depolarization restricts wave propagation (Singer et al., 2001). Here we used a genetic approach to implicate gap junctions in coordinating spontaneous activity in the developing retina.

Extracellular recordings from Cx36–/– mice presented the first evidence that Cx36 influences firing patterns of individual RGCs in the developing retina. Multielectrode array recordings from WT retinas during the first postnatal week (P4–P5) reveal that individual RGCs fire bursts of action potentials that propagate across the retina, which are separated by long periods of silence (Demas et al., 2003; Meister et al., 1991; Torborg et al., 2005). In Cx36–/– retinas, 15% of recorded RGCs have high levels of firing between bursts during the first postnatal week. By P10, RGCs in Cx36–/– retinas still exhibit propagating bursts of action potentials. However, many Cx36–/– cells exhibited spikes between these bursts, whereas WT retinas still have highly correlated bursts with long silent periods (Torborg et al., 2005). This finding is consistent with gap junction coupling being critical for suppressing RGC spiking between retinal waves. The increasing effect of the manipulation on spiking correlates with an increase in Cx36 expression, implying that Cx36-containing gap junctions in AII amacrine cells, cone bipolar cells, and/or RGCs play an increasingly important role as the retina develops.

The persistence of waves during the first postnatal week in Cx36–/– mice is inconsistent with pharmacological blockade of coupling. We postulate that the remaining coordinated activity is mediated in part by gap junctions containing Cx45 (Guldenagel et al., 2000; Maxeiner et al., 2005) or Cx57 (Deans and Paul, 2001; Hombach et al., 2004), the only other neuronal gap junction proteins known to be in the mammalian retina. Indeed, bath application of carbenoxolone (100 μM) blocks the waves that persist at P4, indicating that coupling persists even in the absence of Cx36 (Fig. 4B). However, it is also possible that carbenoxolone inhibits wave propagation by nonspecific actions or that there exists compensation by other mechanisms. Both of these hypotheses are currently under investigation.

Retinal waves during the second postnatal week are mediated by activation of ionotropic glutamate receptors (Bansal et al., 2000; Firth et al., 2005; Syed et al., 2004b; Wong et al., 1998), indicating that coordinated release from bipolar cells is responsible for wave propagation. In contrast to the first postnatal week, when starburst amacrine cells depolarize neighboring starburst amacrine cells (Zheng et al., 2004), there is no evidence of direct bipolar cell–bipolar cell interactions. One possible mechanism for wave propagation during the second postnatal week is that release from bipolar cells is coordinated via AII amacrine cells, which receive glutamatergic input from rod bipolar cells and in turn are gap junction coupled to cone bipolar cells and other AII amacrine cells. The finding that the number of *synchronized* spikes between neighboring RGCs in Cx36–/– mice is indistinguishable from WT (Torborg et al., 2005) indicates that gap junctional coupling via AII amacrine cells is not critical for wave generation.

Compared with the case in WT mice, RGCs in Cx36–/– mice fire many more asynchronous action potentials between correlated bursts. We demonstrated that nearly all action potentials, both correlated and asynchronous, recorded in Cx36–/– mice were blocked by bath application of ionotropic glutamate receptors antagonists (Fig. 5C,D). These findings are surprising, insofar as they indicate that Cx36 functions to regulate spontaneous firing by suppressing release of glutamate between waves. This suppression is not likely to be due to a suppression of glycine release from AII amacrine cells, in that bath application of the glycine receptor antagonist to the WT retina did not reproduce the Cx36–/– phenotype. One possible explanation for how Cx36 functions to suppress glutamate release between waves is that the absence of Cx36 containing gap junctions in cone bipolar cells significantly increases their input resistance and therefore enhances their excitability (Deans et al., 2001; Long et al., 2002). Another possibility is that the absence of Cx36 increases the input resistance of RGCs, thereby making them more sensitive to stimulation by glutamate. Hence gap junctions may be critical for shaping the spontaneous activity patterns not by providing a substrate for wave propagation but rather by regulating the excitability of individual cells that make up the underlying synaptic network.

ACKNOWLEDGMENTS

The authors thank E.J. Chichilnisky for the multielectrode array and technical support, D. Paul for the Cx36–/– mice, Dr. S. Firth for technical assistance, and Dr. T. del Rio for critical reading of the article.

LITERATURE CITED

Bansal A, Singer JH, Hwang BJ, Xu W, Beaudet A, Feller MB. 2000. Mice lacking specific nAChR subunits exhibit dramatically altered spontaneous activity patterns and reveal a limited role for retinal waves in forming ON/OFF circuits in the inner retina. J Neurosci 20:7672–7681.

Belluardo N, Mudo G, Trovato-Salinaro A, Le Gurun S, Charollais A, Serre-Beinier V, Amato G, Haefliger JA, Meda P, Condorelli DF. 2000. Expression of connexin36 in the adult and developing rat brain. Brain Res 865:121–138.

Ben-Ari Y, Khalilov I, Represa A, Gozlan H. 2004. Interneurons set the tune of developing networks. Trends Neurosci 27:422–427.

Bentley D, Keshishian H. 1982. Pathfinding by peripheral pioneer neurons in grasshoppers. Science 218:1082–1087.

Bittman K, Owens DF, Kriegstein AR, LoTurco JJ. 1997. Cell coupling and uncoupling in the ventricular zone of developing neocortex. J Neurosci 17:7037–7044.

Buhl DL, Harris KD, Hormuzdi SG, Monyer H, Buzsaki G. 2003. Selective

impairment of hippocampal gamma oscillations in connexin-36 knockout mouse in vivo. J Neurosci 23:1013–1018.

Catsicas M, Bonness V, Becker D, Mobbs P. 1998. Spontaneous Ca^{2+} transients and their transmission in the developing chick retina. Curr Biol 8:283–286.

Condorelli DF, Parenti R, Spinella F, Trovato Salinaro A, Belluardo N, Cardile V, Cicirata F. 1998. Cloning of a new gap junction gene (Cx36) highly expressed in mammalian brain neurons. Eur J Neurosci 10: 1202–1208.

Condorelli DF, Belluardo N, Trovato-Salinaro A, Mudo G. 2000. Expression of Cx36 in mammalian neurons. Brain Res Brain Res Rev 32:72–85.

Connors BW, Long MA. 2004. Electrical synapses in the mammalian brain. Annu Rev Neurosci 27:393–418.

Cusato K, Bosco A, Rozental R, Guimaraes CA, Reese BE, Linden R, Spray DC. 2003. Gap junctions mediate bystander cell death in developing retina. J Neurosci 23:6413–6422.

Deans MR, Paul DL. 2001. Mouse horizontal cells do not express connexin26 or connexin36. Cell Commun Adhes 8:361–366.

Deans MR, Gibson JR, Sellitto C, Connors BW, Paul DL. 2001. Synchronous activity of inhibitory networks in neocortex requires electrical synapses containing connexin36. Neuron 31:477–485.

Deans MR, Volgyi B, Goodenough DA, Bloomfield SA, Paul DL. 2002. Connexin36 is essential for transmission of rod-mediated visual signals in the mammalian retina. Neuron 36:703–712.

Degen J, Meier C, Van Der Giessen RS, Sohl G, Petrasch-Parwez E, Urschel S, Dermietzel R, Schilling K, De Zeeuw CI, Willecke K. 2004. Expression pattern of lacZ reporter gene representing connexin36 in transgenic mice. J Comp Neurol 473:511–525.

Demas J, Eglen SJ, Wong RO. 2003. Developmental loss of synchronous spontaneous activity in the mouse retina is independent of visual experience. J Neurosci 23:2851–2860.

Famiglietti EV Jr, Kolb H. 1975. A bistratified amacrine cell and synaptic cirucitry in the inner plexiform layer of the retina. Brain Res 84:293–300.

Feigenspan A, Teubner B, Willecke K, Weiler R. 2001. Expression of neuronal connexin36 in AII amacrine cells of the mammalian retina. J Neurosci 21:230–239.

Feigenspan A, Janssen-Bienhold U, Hormuzdi S, Monyer H, Degen J, Sohl G, Willecke K, Ammermuller J, Weiler R. 2004. Expression of connexin36 in cone pedicles and OFF-cone bipolar cells of the mouse retina. J Neurosci 24:3325–3334.

Feller MB. 2002. The role of nAChR-mediated spontaneous retinal activity in visual system development. J Neurobiol 53:556–567.

Feller MB, Wellis DP, Stellwagen D, Werblin FS, Shatz CJ. 1996. Requirement for cholinergic synaptic transmission in the propagation of spontaneous retinal waves. Science 272:1182–1187.

Firth S, Wang C, Feller M. 2005. Retinal waves: mechanisms and function in visual system development. Cell Calcium (in press).

Grubb MS, Thompson ID. 2004. The influence of early experience on the development of sensory systems. Curr Opin Neurobiol 14:503–512.

Guldenagel M, Sohl G, Plum A, Traub O, Teubner B, Weiler R, Willecke K. 2000. Expression patterns of connexin genes in mouse retina. J Comp Neurol 425:193–201.

Gunhan-Agar E, Kahn D, Chalupa LM. 2000. Segregation of On and off bipolar cell axonal arbors in the absence of retinal ganglion cells. J Neurosci 20:306–314.

Hanson MG, Landmesser LT. 2003. Characterization of the circuits that generate spontaneous episodes of activity in the early embryonic mouse spinal cord. J Neurosci 23:587–600.

Haverkamp S, Wassle H. 2000. Immunocytochemical analysis of the mouse retina. J Comp Neurol 424:1–23.

Hidaka S, Kato T, Miyachi E. 2002. Expression of gap junction connexin36 in adult rat retinal ganglion cells. J Integr Neurosci 1:3–22.

Hidaka S, Akahori Y, Kurosawa Y. 2004. Dendrodendritic electrical synapses between mammalian retinal ganglion cells. J Neurosci 24:10553–10567.

Hombach S, Janssen-Bienhold U, Sohl G, Schubert T, Bussow H, Ott T, Weiler R, Willecke K. 2004. Functional expression of connexin57 in horizontal cells of the mouse retina. Eur J Neurosci 19:2633–2640.

Howell BW, Gertler FB, Cooper JA. 1997. Mouse disabled (mDab1): a Src binding protein implicated in neuronal development. EMBO J 16:121–132.

Jeon CJ, Strettoi E, Masland RH. 1998. The major cell populations of the mouse retina. J Neurosci 18:8936–8946.

Kandler K, Katz LC. 1998. Coordination of neuronal activity in developing visual cortex by gap junction-mediated biochemical communication. J Neurosci 18:1419–1427.

Lin JH, Weigel H, Cotrina ML, Liu S, Bueno E, Hansen AJ, Hansen TW, Goldman S, Nedergaard M. 1998. Gap-junction-mediated propagation and amplification of cell injury. Nat Neurosci 1:494–500.

Long MA, Deans MR, Paul DL, Connors BW. 2002. Rhythmicity without synchrony in the electrically uncoupled inferior olive. J Neurosci 22: 10898–10905.

Maxeiner S, Dedek K, Janssen-Bienhold U, Ammermuller J, Brune H, Kirsch T, Pieper M, Degen J, Kruger O, Willecke K, Weiler R. 2005. Deletion of connexin45 in mouse retinal neurons disrupts the rod/cone signaling pathway between AII amacrine and ON cone bipolar cells and leads to impaired visual transmission. J Neurosci 25:566–576.

Meister M, Wong RO, Baylor DA, Shatz CJ. 1991. Synchronous bursts of action potentials in ganglion cells of the developing mammalian retina. Science 252:939–943.

Meister M, Pine J, Baylor DA. 1994. Multi-neuronal signals from the retina: acquisition and analysis. J Neurosci Methods 51:95–106.

Menger N, Pow DV, Wassle H. 1998. Glycinergic amacrine cells of the rat retina. J Comp Neurol 401:34–46.

Mills SL, O'Brien JJ, Li W, O'Brien J, Massey SC. 2001. Rod pathways in the mammalian retina use connexin 36. J Comp Neurol 436:336–350.

Moon JI, Kim IB, Gwon JS, Park MH, Kang TH, Lim EJ, Choi KR, Chun MH. 2005. Changes in retinal neuronal populations in the DBA/2J mouse. Cell Tissue Res 320:51–59 [Epub 2005 Feb 2016].

Naus CC, Bani-Yaghoub M. 1998. Gap junctional communication in the developing central nervous system. Cell Biol Int 22:751–763.

Peinado A, Yuste R, Katz LC. 1993. Gap junctional communication and the development of local circuits in neocortex. Cereb Cortex 3:488–498.

Penn AA, Riquelme PA, Feller MB, Shatz CJ. 1998. Competition in retinogeniculate patterning driven by spontaneous activity. Science 279: 2108–2112.

Personius KE, Balice-Gordon RJ. 2001. Loss of correlated motor neuron activity during synaptic competition at developing neuromuscular synapses. Neuron 31:395–408.

Pourcho RG, Goebel DJ. 1985. A combined Golgi and autoradiographic study of (^{3}H)glycine-accumulating amacrine cells in the cat retina. J Comp Neurol 233:473–480.

Pow DV, Hendrickson AE. 2000. Expression of glycine and the glycine transporter glyt-1 in the developing rat retina. Vis Neurosci 17:1–9.

Rash JE, Staines WA, Yasumura T, Patel D, Furman CS, Stelmack GL, Nagy JI. 2000. Immunogold evidence that neuronal gap junctions in adult rat brain and spinal cord contain connexin-36 but not connexin-32 or connexin-43. Proc Natl Acad Sci U S A 97:7573–7578.

Rice DS, Curran T. 2000. Disabled-1 is expressed in type AII amacrine cells in the mouse retina. J Comp Neurol 424:327–338.

Saint-Amant L, Drapeau P. 2001. Synchronization of an embryonic network of identified spinal interneurons solely by electrical coupling. Neuron 31:1035–1046.

Schubert T, Degen J, Willecke K, Hormuzdi SG, Monyer H, Weiler R. 2005. Connexin36 mediates gap junctional coupling of alpha-ganglion cells in mouse retina. J Comp Neurol 485:191–201.

Sernagor E, Eglen SJ, Wong RO. 2001. Development of retinal ganglion cell structure and function. Prog Ret Eye Res 20:139–174.

Singer JH, Mirotznik RR, Feller MB. 2001. Potentiation of L-type calcium channels reveals nonsynaptic mechanisms that correlate spontaneous activity in the developing mammalian retina. J Neurosci 21:8514–8522.

Sohl G, Degen J, Teubner B, Willecke K. 1998. The murine gap junction gene connexin36 is highly expressed in mouse retina and regulated during brain development. FEBS Lett 428:27–31.

Sohl G, Guldenagel M, Traub O, Willecke K. 2000. Connexin expression in the retina. Brain Res Brain Res Rev 32:138–145.

Syed MM, Lee S, He S, Zhou ZJ. 2004a. Spontaneous waves in the ventricular zone of developing mammalian retina. J Neurophysiol 91: 1999–2009 [Epub 2003 Dec 1917].

Syed MM, Lee S, Zheng J, Zhou ZJ. 2004b. Stage-dependent dynamics and modulation of spontaneous waves in the developing rabbit retina. J Physiol 560:533–549 [Epub 2004 Aug 2012].

Torborg C, Hansen K, Feller M. 2005. High frequency, synchronized bursting drives eye-specific segregation of retinogeniculate projections. Nat Neurosci 8:72–78.

Vaney DI, Nelson JC, Pow DV. 1998. Neurotransmitter coupling through gap junctions in the retina. J Neurosci 18:10594–10602.

Veruki ML, Hartveit E. 2002a. AII (Rod) amacrine cells form a network of electrically coupled interneurons in the mammalian retina. Neuron 33:935–946.

Veruki ML, Hartveit E. 2002b. Electrical synapses mediate signal transmission in the rod pathway of the mammalian retina. J Neurosci 22:10558–10566.

Vessey JP, Lalonde MR, Mizan HA, Welch NC, Kelly ME, Barnes S. 2004. Carbenoxolone inhibition of voltage-gated Ca channels and synaptic transmission in the retina. J Neurophysiol 92:1252–1256 [Epub 2004 Mar 1217].

Wong RO, Meister M, Shatz CJ. 1993. Transient period of correlated bursting activity during development of the mammalian retina. Neuron 11:923–938.

Wong RO, Chernjavsky A, Smith SJ, Shatz CJ. 1995. Early functional neural networks in the developing retina. Nature 374:716–718.

Wong WT, Sanes JR, Wong ROL. 1998. Developmentally regulated spontaneous activity in the embryonic chick retina. J Neurosci 18:8839–8852.

Yuste R, Nelson DA, Rubin WW, Katz LC. 1995. Neuronal domains in developing neocortex: mechanisms of coactivation. Neuron 14:7–17.

Zhang M, Xin H, Roon P, Atherton SS. 2005. Infection of retinal neurons during murine cytomegalovirus retinitis. Invest Ophthalmol Vis Sci 46:2047–2055.

Zheng JJ, Lee S, Zhou ZJ. 2004. A developmental switch in the excitability and function of the starburst network in the mammalian retina. Neuron 44:851–864.

Zhou ZJ. 2001a. A critical role of the strychnine-sensitive glycinergic system in spontaneous retinal waves of the developing rabbit. J Neurosci 21:5158–5168.

Zhou ZJ. 2001b. The function of the cholinergic system in the developing mammalian retina. Prog Brain Res 131:599–613.